

MSN0004

Influence of Surface Roughness to Tool Run-out with Ball Endmill

Shin Nakai^{1,*}, Yukio Maeda¹, Daisuke Goto¹, Kazuya Kato², Hideaki Tanaka², Takanori Yazawa³,
and Tatsuki Otsubo⁴

¹Toyama Prefectural University, 5180 Kurokawa, Imizu-shi, Toyama 939-0398, Japan

²Shonan Institute of Technology, 1-1-25 Tsujido-nishikaigan, Fujisawa-shi, Kanagawa, 251-0046, Japan

³Nagasaki University, 1-14 Bunkyo-machi, Nagasaki-shi, Nagasaki, 852-8521, Japan

⁴Salesian Polytechnic, 4-6-8 Oyamagaoka, Matida-shi, Tokyo, 194-0215, Japan

* Shin Nakai: bb34sna@gmail.com, +81-766-56-7500, +81-766-56-8030

Abstract

Micro-channel chips are used in micro total analysis systems and have been attracting attention in the medical field recently. In general, photolithography technology is used in semiconductor manufacturing to construct micro-channel chip dies. However, this technology requires specific resources, such as expensive clean room facilities, and numerous manufacturing processes, such as photomask fabrication, which involves the application of a photoresist to a substrate. The purpose of this study is to develop processing technology capable of manufacturing micro-channel chip dies through the process of micro endmilling. We disclosed discovered that tool run-out on the order of several micrometers during micro-groove milling reduced machining accuracy and shortened tool lifespan short. Therefore, we experimentally examined a method for reducing the influence of tool run-out on machining accuracy with two-tooth and ball endmills by modifying the tool setting angle. In addition, the relationship between the angle of the cutting edge and the cutting action area in slant milling was also examined. As a result, the modifying the tool setting angle improved the surface roughness of side of groove and reduced the change in the cutting force for two-tooth endmilling. In addition, the modified tool setting angle was able to reduce the influence of groove width of tool run-out by up to 10 percent. In ball end milling, modifying the tool setting angle reduced the influence of tool run-out on machining accuracy. In addition, cutting marks were not formed in the up cut side when the angle of the cutting edge was larger than the maximum amount of undeformed chip thickness.

Keywords: Micro-channel chip, Milling, Micro-groove, Tool run-out, Micro endmill

1. Introduction

Recently, the use of micro-channel chips [1-4] in micro total analysis systems (Fig. 1) has been attracted attention in the medical field. Figure 2 shows an example of a micro-channel. Micro-channel chips have micro-grooves 100 μm wide and 50 μm deep, as shown in Fig. 2. Photolithography, which is used in semiconductor manufacturing, is also employed for manufacturing micro-channel chip Si-dies [5-7]. However, this technology requires the use of numerous manufacturing processes and resources, such as mask fabrication and the application of a photoresistor to a substrate, as well as expensive clean room facilities [8, 9]. Figure 3 shows a schematic view of the machining process. When a micro-groove is formed by machining with a micro endmill, the main process is reduced to only three steps. Machining does not require an expensive clean room. Microchannel dies need to be manufactured to high accuracy. This study examines how to form a fine groove by using a micro endmill with the aim of shortening lead-time and reducing cost. A previous study by the same authors showed that tool run-out on the order of several micrometers experienced during micro-groove milling reduced machining accuracy and tool life [10-15]. This study examines the influence of a ball endmill tool run-out on machining accuracy, and how to reduce this influence.

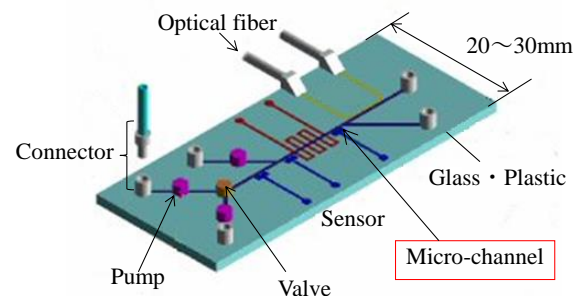


Fig.1 Basic concept of a micro total analysis system

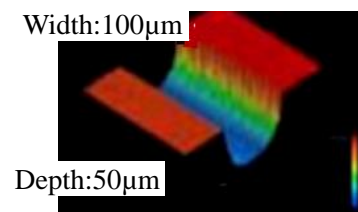


Fig.2 Example of a micro-channel

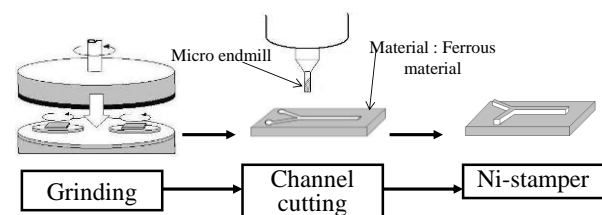


Fig.3 Schematic of the machining process

MSN0004

2. Experimental Equipment and Conditions

Figure 4 shows the relationship between the tool run-out and the locus of the cutting edges with micro endmill. Figure 4(a) shows that when the tool setting angle is $\lambda = 0^\circ$, the cutting edge is mounted in the radial direction of the tool and points towards the locus of the tool run-out. At this time, cutting edge ① makes a wide rotation and cutting edge ② makes a narrow rotation. Figure 4(b) shows that when the tool setting angle is $\lambda = 90^\circ$, the cutting edge is set in a direction tangential to the tool and points toward the locus of the tool run-out. With this, the loci of the cutting edges of the two pieces correspond with one other. Therefore, by matching the tool setting angle with the tangential direction, it is possible to significantly reduce the influence of the tool run-out on machining accuracy with a two-tooth square endmill.

It is possible to calculate the effective tool diameter d' by using Eq. (1). With the tool setting angle $\lambda = 90^\circ$, it is possible to calculate the effective tool diameter d'_{90° is possible to calculate by using Eq. (2). Figure 5 shows the relationship between the tool run-out and the effective tool diameter with a tool setting angle $\lambda = 90^\circ$. Figure 5 shows that the effective tool diameter increases with an increase in the tool run-out. For example, if the tool diameter is $d = 0.5$ mm and the tool run-out is $\delta = 10$ μm , the effective tool diameter is 510.0 μm with the tool setting angle of $\lambda = 0^\circ$. In contrast, the effective tool diameter is 500.1 μm with a tool setting angle $\lambda = 90^\circ$. Therefore, a tool setting angle $\lambda = 90^\circ$ can reduce the influence of tool run-out to less than 1/10. In addition, it is possible to calculate the effective tool run-out δ' is possible to calculate by using Eq. (3). Figure 6 shows the relationship between tool run-out and tool setting angle as seen from Eq. (3), when tool diameter of the endmill is $\phi 0.5$ mm and the tool run-out δ is 10 μm . From Fig. 6, if the tool setting angle is modified to $\lambda = 90^\circ \pm 5^\circ$, it is possible to obtain an effective tool diameter less than 1 μm . Therefore, it is possible to reduce the influence of tool run-out on machining accuracy by modifying the tool setting angle. This is similar to the ball endmilling process.

The experimental equipment and conditions used in this study are shown in Table 1. The machine tool used was an NC milling machine (WAIDA MCX-10). The micro-channel chip dies used workpieces made of SUS316 steel. During machining, oil was sprayed onto the workpiece at a rate of 21 mL/h using a mist spray unit (EVERLOY MD-1), and the cutting force was measured by a dynamometer (KISTLER Type9251A) placed under the workpiece.

$$d' = \sqrt{d^2 + \delta^2 + 2d\delta \cos \lambda} \quad (1)$$

$$d'_{90^\circ} = \sqrt{d^2 + \delta^2} \quad (2)$$

$$\delta' = d' - d \quad (3)$$

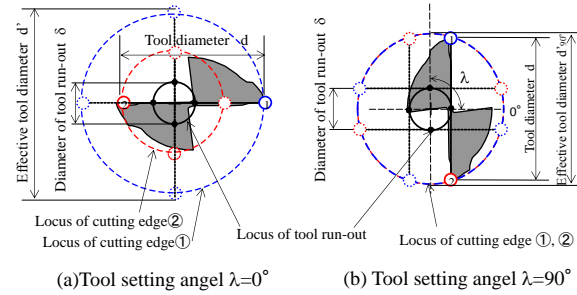


Fig.4 Relationship between tool run-out and locus of cutting edges for endmilling

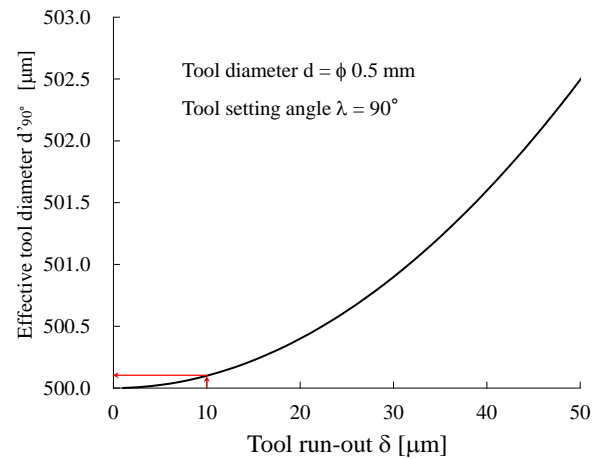


Fig.5 Relationship between tool run-out and effective tool diameter with tool setting angle of $\lambda = 90^\circ$

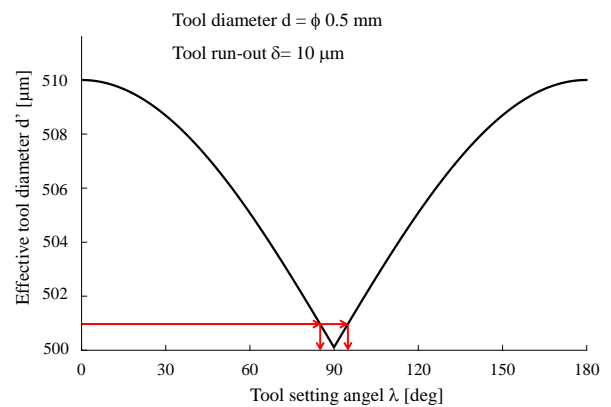


Fig.6 Relationship between tool run-out and tool setting angle

MSN0004

Table.1 Experimental equipment and conditions

Machine tool	NC milling machine(MCX-01 WAIDA)
Cutting tool	Micro endmill($\phi 0.5$ mm 2NT) Micro ball endmill(R0.25 mm 2NT)
Workpiece	SUS316 *4×120×H 7 mm
Cutting conditions	$N = 48,000 \text{ min}^{-1}$ $F = 480 \text{ mm/min}$ $S_z = 5 \text{ }\mu\text{m/tooth}$ $Ad = 50 \text{ }\mu\text{m}$ $\delta = 8 - 10 \text{ }\mu\text{m}$
Lubricating system	MQL equipment: MD-1 Kyoritsu Gokin Corporation (Flow-rate = 21 mL/h, Air Pressure = 0.1 MPa)

3. Experimental Results

3.1 Influence of Groove Side on Tool Run-out

Figure 7 shows a schematic of the experimental setup. Tool run-out was measured using a precision capacitive sensor (MicroSense Model 4830) before milling. The concentricity of the tool center and the peripheral cutting edge was less than $0.1 \text{ }\mu\text{m}$. After milling, the side of the groove that was formed on the workpiece and was observed using a confocal microscope. The cutting forces were measured in the feed direction F_x and the vertical direction F_y to F_x , as shown in Fig. 7. Figure 8 shows the relationship between the tool rotation angle in one rotation, and the cutting force of endmill. Figure 8 shows that with a tool setting angle of $\lambda = 0^\circ$, the waveform of the cutting force corresponding to cutting edge ② was scarcely observed, because the undeformed chip thickness increases in cutting edge ① and decreases in cutting edge ②. On the other hand, when the tool setting angle was $\lambda = 90^\circ$, it was observed that the waveform of the cutting force corresponding to cutting edge ② is the same level as that of ①. Therefore, the cutting edges were shown to affect endmilling. Figure 9 shows photographs of the side of the groove made with the endmill. The cutting marks were formed every $10 \text{ }\mu\text{m}$ corresponding to one tool rotation, and were observed on the down-cut side. In addition, the surface roughness of the groove side was measured in the direction shown in Fig. 9. Figure 10 shows the result of measuring the surface roughness. Figure 10 shows that the surface roughness was better with a tool setting angle $\lambda = 90^\circ$ than with a tool setting angle $\lambda = 0^\circ$.

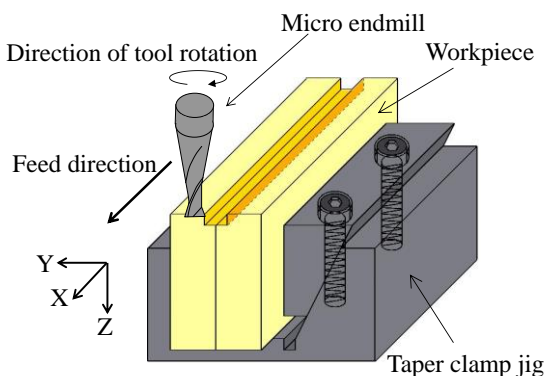


Fig.7 Schematic of experimental setup

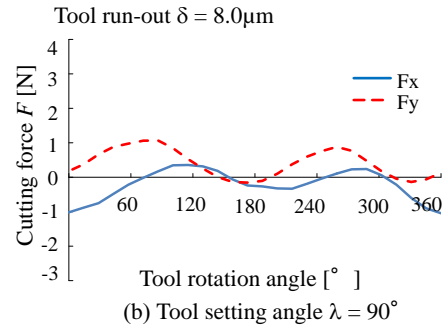
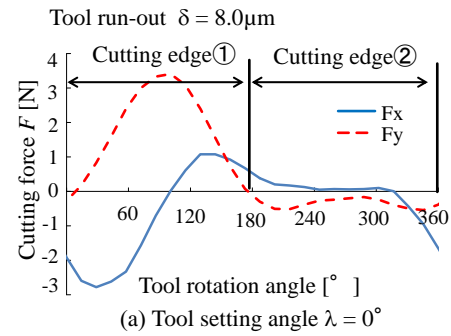


Fig.8 Relationship between tool rotation angle and cutting forces with endmill

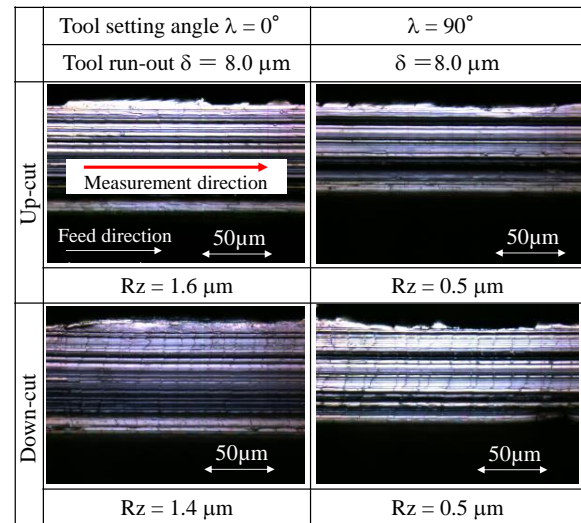


Fig.9 Photographs of groove side with endmill

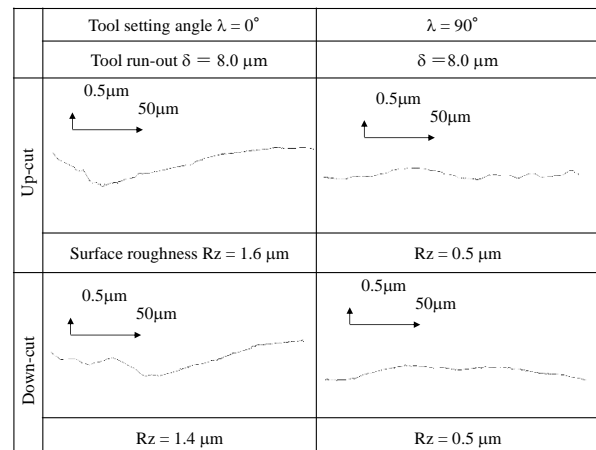


Fig.10 Profiles of surface roughness with endmill

MSN0004

3.2 Influence of Surface Roughness to Tool Run-out with Ball Endmill

We examined that modifying the tool setting angle reduced the influence of tool run-out on machining accuracy in a manner similar to that in ball end milling. Figure 11 shows the relationship between tool run-out and the locus of cutting edges with a ball endmill. As shown in Fig. 11(b), the tool setting angle is $\lambda = 90^\circ$ when the cutting edge is set in a direction tangential to the tool, towards the locus of tool run-out. With this, the loci of the cutting edges of the two pieces correspond with each other. Therefore, by modifying tool setting angle to $\lambda = 90^\circ$, it is possible to significantly reduce the influence of tool run-out on machining accuracy with a ball endmill. Figure 12 shows the relationship between the tool rotation angle and cutting forces by using a ball endmill. With a tool setting angle of $\lambda = 0^\circ$, the waveform of the cutting force corresponding to cutting edge ② was scarcely observed. On the other hand, with a tool setting angle of $\lambda = 90^\circ$, it was observed that the waveform of the cutting force corresponding to cutting edge ② was the same level as that of ①. Figure 13 shows photographs of the groove with a ball endmill. With a tool setting angle of $\lambda = 0^\circ$, the groove width increased approximately $8 \mu\text{m}$ corresponding to tool run-out. However, with a tool setting angle $\lambda = 90^\circ$, the groove width was close to its theoretical value. The surface roughness of the groove was measured in the direction shown in Fig. 14. Figure 14 shows the measured surface roughness results. Figure 14 illustrates that the surface roughness of the groove of the up-cut side was bad. However, the surface roughness of grooves on the up-cut and down-cut sides were better with a tool setting angle of $\lambda = 90^\circ$ than with a tool setting angle of $\lambda = 0^\circ$.

From Fig. 13, the cutting marks that were formed every $10 \mu\text{m}$ corresponding to one tool rotation were observed on the down-cut side. There were differences between cutting marks on the up-cut and down-cut sides. In addition, we examined cutting action area by slant milling. Figure 15 shows a schematic of slant milling with a ball endmill. Cutting marks were formed at axial depth of cut (A_d) is more than $10 \mu\text{m}$ in the up-cut side by observing machined surface. However, they were not formed at axial depth of cut (A_d) is less than $10 \mu\text{m}$. We examined this cause from relationship between undeformed-chip thickness and cutting edge radius (R). Figure 16 shows the measured results of the cutting edge radius (R) with ball endmill. The measured result of cutting edge radius (R) was $1.5 \mu\text{m}$. Figure 17 shows the schematic of the undeformed-chip thickness with a ball endmill. When the depth of cut (A_d) is tinier than the radius of the tool (r), undeformed-chip thickness can be calculated using Eq. (4). Figure 18 shows photographs of the groove surface with a ball endmill in slant milling. When the depth of cut is $10 \mu\text{m}$, the undeformed-chip thickness is $1.4 \mu\text{m}$ using Eq. (4). We considered

cutting that undeformed-chip thickness was smaller than cutting edge R was cutting of rubbing area that wasn't formed cutting marks in the up-cut side, because cutting marks was formed in $A_d \leq 10 \mu\text{m}$ from Fig. 18. Furthermore, cutting marks that were formed every $10 \mu\text{m}$ corresponding to one tool rotation in the down-cut side. They were formed in spite of depth of cut (A_d).

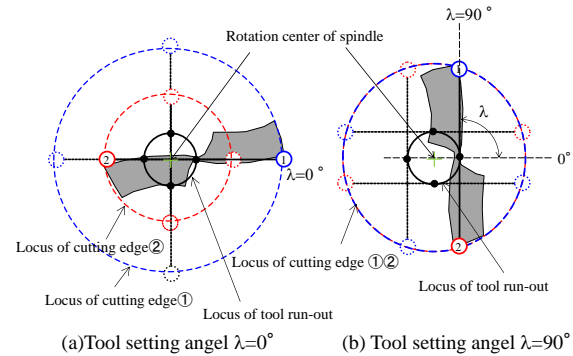


Fig.11 Relationship between tool run-out and locus of cutting edges for a ball endmilling

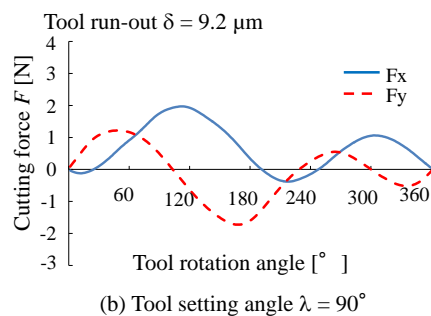
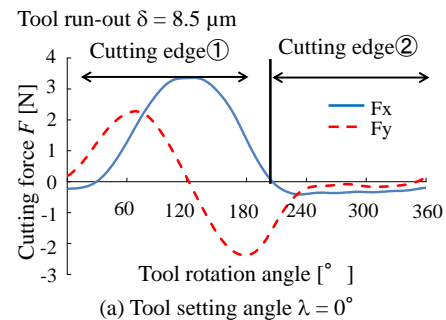


Fig.12 Relationship between tool rotation angle and cutting forces with ball endmill

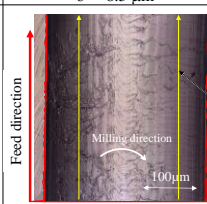
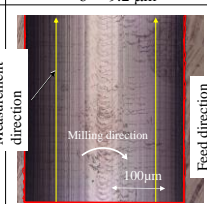
Tool setting angle	$\lambda = 0^\circ$		$\lambda = 90^\circ$	
Tool run-out	$\delta = 8.5 \mu\text{m}$		$\delta = 9.2 \mu\text{m}$	
Photograph of work piece				
	Up-cut	Down-cut	Up-cut	Down-cut
Surface roughness	$1.0 \mu\text{mRz}$	$0.4 \mu\text{mRz}$	$0.9 \mu\text{mRz}$	$0.4 \mu\text{mRz}$
Groove width theoretical	301.6 μm		304.7 μm	
Groove width experimental	309.3 μm		306.1 μm	

Fig.13 Photographs of groove with ball endmill

MSN0004

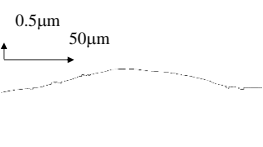
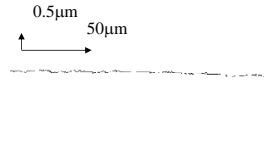
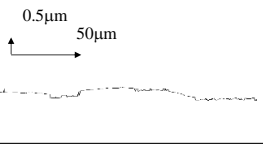
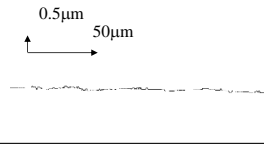
	Tool setting angle $\lambda = 0^\circ$	$\lambda = 90^\circ$
	Tool run-out $\delta = 8.5 \mu\text{m}$	$\delta = 9.2 \mu\text{m}$
Up-cut		
	Surface roughness $R_z = 1.0 \mu\text{m}$	$R_z = 0.4 \mu\text{m}$
Down-cut		
	Surface roughness $R_z = 0.9 \mu\text{m}$	$R_z = 0.4 \mu\text{m}$

Fig.14 Profiles of the surface roughness with ball endmill

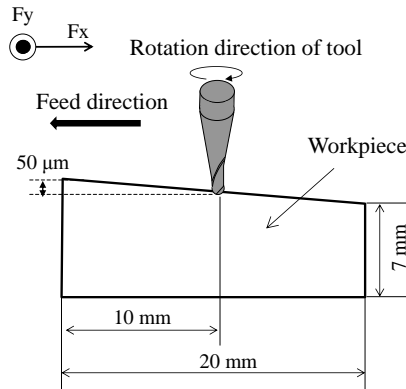


Fig.15 Schematic of slant milling with ball endmill

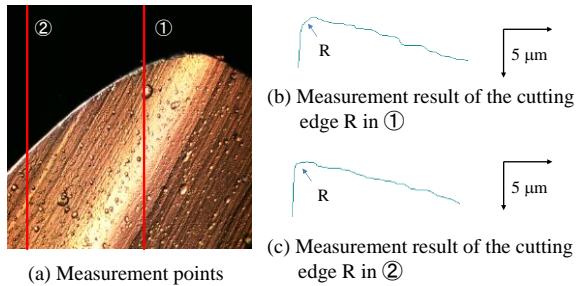


Fig. 16 Measurement results for cutting edge R with a ball endmill

h_{\max} : Maximal undeformed-chip thickness, S_z : Feed per tooth
 r : Radius of the tool, Ad : Depth of cut, θ : The angle of h_{\max}

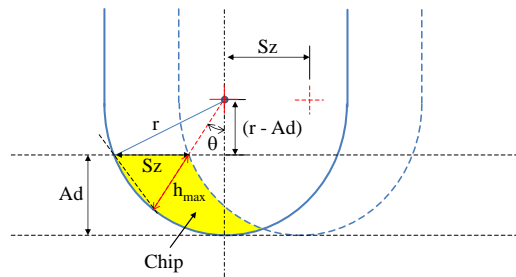
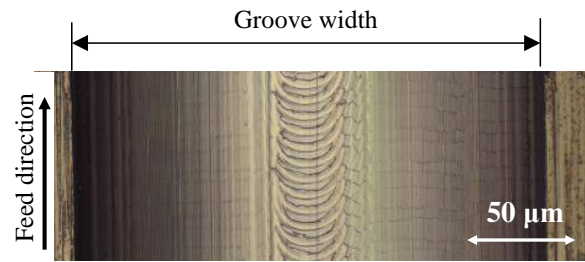
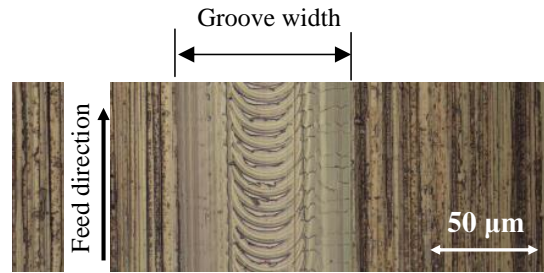


Fig.17 Schematic of undeformed-chip thickness with ball endmill

$$h_{\max} = S_z \cdot \sin \theta, \quad \theta = \cos^{-1} \left(\frac{r - Ad}{r} \right) \quad (4)$$



(a) $Ad=50 \mu\text{m}$ ($h_{\max}=3.0 \mu\text{m}$)



(b) $Ad=5 \mu\text{m}$ ($h_{\max}=1.0 \mu\text{m}$)

Fig.18 Photographs of groove surface with ball endmill in slant milling

4. Conclusions

We examined influence of ball endmill tool run-out to machining accuracy and its improvement method. The following conclusions were drawn from the results.

- (1) For the endmilling, a tool setting angle of $\lambda = 90^\circ$, the changes of cutting forces were reduced and the surface roughness was good.
- (2) With the ball endmilling, changes in cutting forces were reduced and the surface roughness was good same as endmilling when tool setting angle was modified to $\lambda = 90^\circ$.
- (3) For the ball endmilling, cutting marks wasn't formed in the up-cut side when undeformed-chip thickness was smaller than cutting edge radius (R).

5. References

- [1] K. Iwatsuka, Y. Maeda, H. Tanaka, T. Yazawa, and S. Suzuki. (2014). Effect of Tool Run-Out on Micro-Groove Milling for a Micro-channel Die International Journal of Automation Technology, Vol.8, No.2, pp. 275–281.
- [2] T. Kitamori. (2009). Microchip Analysis and Synthesis Systems, Trends in Academic, Vol.14, No.3, pp.42-45.
- [3] M. Esashi. (2009). Micromachine /MEMS, Journal of the Japan Society for Precision Engineering, Vol.75, No1, pp.78-79 (in Japanese).

MSN0004

- [4] A. Manz, J.C. Fettinger, E. Verpoorte, H. Ludi, H.M. Widmer and D.J. Harrison. (1991). Micromachining of monocrystalline silicon and glass for chemical analysis systems A look into next century's technology or just a fashionable craze, *TrAC Trends in Analytical Chemistry*, Vol.10, pp.144-149.
- [5] M. Tokeshi. (2005). Glass chip manufacturing method using a semiconductor microfabrication technology, *Electronic materials*, pp.26-28 (in Japanese).
- [6] J. H. Parka, N.-E.Leea,J.SParkb, and H. D. PArkb. (2005). Deep dry etching of borosilicate glass using SF₆/Ar inductively coupled plasma, *Microelectronic Engineering*, Vol.82, pp. 119-128.
- [7] K. Iwatsuka, Y. Maeda, H. Tanaka, T. Yazawa, and S. Suzuki. (2011). Study on micro-groove milling of a micro-channel die—Selection guidelines for cutting conditions with micro end mills—, *Proceedings of the 6th International Conference on Leading Edge Manufacturing in 21st century (LEM21)*, pp. 32–73.
- [8] Y. Maeda, K. Iwatsuka, Y. Isokawa, T. Yazawa, Y. Fukuda and S. Suzuki. (2010). Study on fine-groove milling of micro-channel die—Surface roughness and form accuracy of fine groove—, *The 8th Manufacturing & Machine too Conference*, pp. 249–250 (in Japanese).
- [9] H. Ogawa, M. Masuda, A. Akira, Y. Kogami. (2006). Effect of Cavitation of Cutting Fluid in Micro Drilling (1st Report), *Journal of the Japan Society for Precision Engineering*, pp. 626–630 (in Japanese).
- [10] H. Ogawa, M. Masuda, A. Akira, Y. Kogami. (2007). Relation between Drilling Conditions and Tool Life in Micro Drilling (2nd Report), *Journal of the Japan Society for Precision Engineering*, pp. 578–582 (in Japanese).
- [11] G. Bissacco, H. N. Hansen, J. Slunsky. (2008). Modelling the cutting edge radius size effect for force prediction in micro milling, *CIRP – Manufacturing Technology*, Vol.57, pp.113-116.
- [12] C. Y. Huang, J. J. Junz Wang. (2007). Mechanistic Modeling of Process Damping in Peripheral Milling, *Transactions of the ASEM*, Vol.129, pp.12-19.
- [13] Jean Philippe Costes. (2011). Vincent Moreau, Surface roughness prediction in milling based on tool displacements, *Journal of Manufacturing Processes*, Vol.13, pp.133-140.
- [14] Boxiao Ma, Mituyoshi Nomura, Takahiro Kawashima, Osamu Horiuchi. (2008). Study on Micro Drilling –Rotating Bending Fatigue of Micro Carbide Drills-, *Engineering Materials*, Vol.407, pp.45-48.
- [15] N. T. Nguyen and S. T. Wereley. (2006). “Fundamentals and Applications of Microfluidics,” Artech House, 2nd edition.